01 Nov 2023

Development Of Eco-friendly Chitosan-g-polyacrylamide Preformed Particle Gel For Conformance Control In High-temperature And High-salinity Reservoirs

Reem Elaf

Ahmed Ben Ali

Mohammed Saad

Ibnelwaleed A. Hussein

et. al. For a complete list of authors, see https://scholarsmine.mst.edu/geosci_geo_peteng_facwork/2167

Recommended Citation

R. Elaf et al., "Development Of Eco-friendly Chitosan-g-polyacrylamide Preformed Particle Gel For Conformance Control In High-temperature And High-salinity Reservoirs," *Geoenergy Science and Engineering*, vol. 230, article no. 212136, Elsevier, Nov 2023.
The definitive version is available at https://doi.org/10.1016/j.geoen.2023.212136

230 (2023) 212136

Contents lists available at ScienceDirect

Geoenergy Science and Engineering

journal homepage: www.sciencedirect.com/journal/geoenergy-science-and-engineering

Development of eco-friendly chitosan-g-polyacrylamide preformed particle gel for conformance control in high-temperature and high-salinity reservoirs

Reem Elaf [a], Ahmed Ben Ali [a], Mohammed Saad [a,b,**], Ibnelwaleed A. Hussein [a,b,*], Baojun Bai [c]

[a] Gas Processing Center, College of Engineering, P.O. Box 2713, Qatar University, Doha, Qatar
[b] Department of Chemical Engineering, College of Engineering, P.O. Box 2713, Qatar University, Doha, Qatar
[c] Department of Geosciences and Geological and Petroleum Engineering, Missouri University of Science and Technology, Rolla, MO, 65409, USA

ARTICLE INFO

Keywords:
Chitosan
Swelling ratio
Mechanical strength
Thermal stability
Conformance control
Grafted polysaccharides

ABSTRACT

Oil and gas extraction has become challenging nowadays due to the accompanying amount of excess produced water that results in poor recoverability of hydrocarbon, besides other environmental and economic isues. A recent and efficient technology for conformance control is the injection of preformed particle gels (PPGs), which results in a more practical production process. Nevertheless, existing treatments fail in high-temperature reservoirs, are extremely sensitive to salinity, and are hazardous. The characteristics of the designed PPG, such as mechanical strength and thermal durability, is mainly depend on their crosslinking method. Polysaccharides-based gels prepared by physical crosslinking are weaker than the ones crosslinked by strong covalent bonding. This paper uses one of the polysaccharides and proposes an environmentally friendly PPG for water shutoff applications in reservoirs of high temperature (≤130 °C) and high salinity (200,000 ppm), named chitosan grafted polyacrylamide crosslinked with N, N′-methylene bisacrylamide, synthesized chemically by microwave assisted method. The PPG's chemical compositions, grafting and crosslinking mechanism have been investigated by FTIR spectroscopy and SEM techniques. Swelling kinetics, swelling capacity, and mechanical strength measurements were conducted in different conditions to evaluate the influence of the reservoir conditions, such as salinity, temperature, and pH, on the PPG stability. TGA experiments were also performed to examine the thermal stability. Results have shown that the grafting method has produced a PPG with improved mechanical strength, thermal durability, and salt insensitivity. These results are consistent with the testing observations, where the swelling capacities and the storage modulusof Cs/PAMBA samples, with different MBA content, in deionized water were 2.72–11.64 g/g and 4272.1–22,687 Pa, respectively, while they are 2.52–13.82 g/g and 3699.6–22,910, respectively, in saline solution of TDS 67.2976 g/L. The PPGs are thermally stable and resist temperatures up to 130 °C. Besides being eco-friendly, the Cs/PAMBA showed good long-term thermal stability in high-temperature and high-salinity environments.

1. Introduction

The generation of excess produced water has become a problem in the oil industry, leaving a considerable amount of unrecoverable hydrocarbon in a reservoir. Excess water production reduces the well lifetime (Sagbana and Abushaikha, 2021) and triggers corrosion, scale deposition, and increases the load on surface facilities (Seright and Brattekas, 2021). According to the latest statistics, 210 million barrels of produced water versus 75 million barrels of oil are generated daily worldwide (Yang et al., 2022). The unwanted water usually originates from active aquifers or comes in conjunction with oil production during the last stage of the water flooding process (Taha and Amani, 2019). For instance, when the production well is connected to an aquifer through an open fracture or when the water injection well just happens to be connected to the production well via an open fracture (also known as thief zones), as shown in Fig. 1. Polymeric formulations such as preformed particle gel (PPG), foamed gel, and in-situ crosslinked gel have proved their potential application in sealing high permeability and/or

* Corresponding author. Gas Processing Center, College of Engineering, P.O. Box 2713, Qatar University, Doha, Qatar.
** Corresponding author. Gas Processing Center, College of Engineering, P.O. Box 2713, Qatar University, Doha, Qatar.
E-mail addresses: m.saleh@qu.edu.qa (M. Saad), ihussein@qu.edu.qa (I.A. Hussein).

https://doi.org/10.1016/j.geoen.2023.212136
Received 21 May 2023; Received in revised form 27 June 2023; Accepted 9 July 2023
Available online 13 July 2023

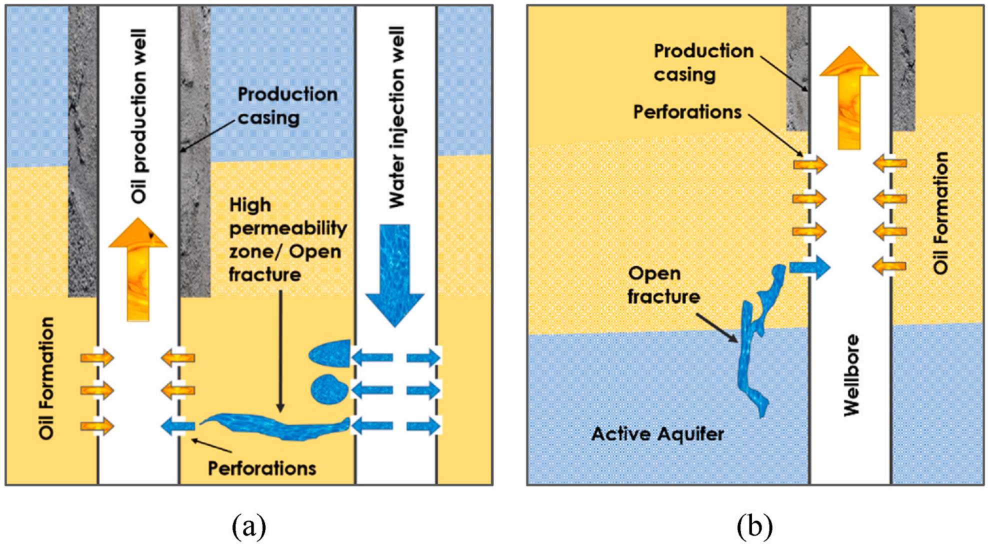

Fig. 1. Examples of unwanted water types: (a) through flooding process and (b) through active aquifer.

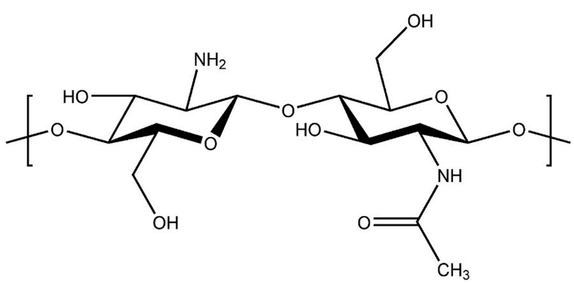

Fig. 2. Chemical structure of Chitosan (Cs).

Table 1
The compositions grafted materials.

Materials	Cs (g)	APS (g)	AM (g)	MBA (g)
Cs/PAMBA$_{0.25\%}$	2	0.4	20	0.05
Cs/PAMBA$_{1\%}$	2	0.4	20	0.2
Cs/PAMBA$_{5\%}$	2	0.4	20	1
Cs/PAMBA$_{25\%}$	2	0.4	20	5

Table 2
The chemical composition of the Brine solutions.

Salts	Brine A	Brine B	Brine C
	Concentration (g/L)		
$NaHCO_3$	0	0.2382	2.015
Na_2SO_4	0	6.5754	2.587
$CaCl_2{\cdot}H_2O$	0	2.3945	6.098
$MgCl_2{\cdot}6H_2O$	0	18.0539	49.599
NaCl	10.0	40.2738	137.273
$CaCO_3$	0	0	1.628
KCl	0	0	0.8
TDS	10.0	67.2976	200

fractured zones. In addition, they are used for conformance control to enhance CO_2 flooding sweep efficiency and storage efficiency (Sun et al., 2020).

The preformed particle gel, a more recent technique, is created in surface facilities outside the reservoirs to produce dried particle gels that are then injected into the targeted zones in the reservoirs and swell by soaking up water as superabsorbent polymers, thereby plugging the fractured zone and improving the oil recovery.

Numerous studies have recently examined the mechanism of PPG propagation and PPG performance in high-permeability channels and fractures, including their swelling ratio and mechanical strength, with particular emphasis on the effects of particle size, PPG composition (e.g., monomer/polymer, crosslinker, and initiator concentrations), and reservoir conditions (e.g., temperature, salinity, and pH) (Farasat et al., 2017), (Bai et al., 2007), (Lenji et al., 2018b). In addition, other studies have included thermal stability and aging tests, such as TGA, DSC, etc., to ensure that the PPGs can retain 80% of their original structure and strength at specified temperatures for prolongated time (Bai et al., 2007), (Oppong et al., 2023), (Wang et al., 2017). Current well-known PPG formulations frequently investigated in the literature consist of synthetic polymers such as polyacrylamide, polyacrylic acid, and the copolymer combining the two crosslinked with organic crosslinkers such as N, N′-methylene-bisacrylamide (MBA) (Farasat et al., 2017), (Farasat et al., 2021), (Cheng et al., 2022), (Heidari et al., 2021), (Heidari et al., 2019a), (Oppong et al., 2022), (Baloochestanzadeh et al., 2021). Other polymers, such as sulfonated polyacrylamide are crosslinked with inorganic crosslinkers, including aluminum nitrate nanohydrate (Lenji et al., 2018b), chromium acetate (Heidari et al., 2019b), and polyethyleneimine (Aqcheli et al., 2020).

The research and development of water shutdown techniques have recently been intensified, and this has included addressing and overcoming the deficiencies of the designed PPGs to make them appropriate for challenging reservoir conditions. For example, Paprouschi et al. (2021) developed a thermally resistant PPG to a temperature of up to 80 °C with a storage modulus of less than 1000 Pa by introducing graphene nanoplatelets into their formulation (Paprouschi et al., 2021). Baloochestanzadeh et al. (2021) developed a PPG made of starch grafted crosslinkked PAM loadded with silica nanoparticles, which was tolerable to a temperature of 90 °C and a TDS of 225,000 ppm with a mechanical strength of 900 Pa (Baloochestanzadeh et al., 2021). However, these PPGs may degrade at temperatures above 90 °C due to their insufficient strength to sustain long-term thermal stability. In addition, although Lenji et al., 2018b have developed highly swellable PPGs with a 50 g/g ratio at a TDS of 209,433 ppm; yet, they have degraded at temperatures above 80 °C and are extremely sensitive to salinity (Lenji et al., 2018b). Other investigations, such as a PPG made up of sulfonated polyacrylamide with chromium acetate, claimed a high gel strength of about 35.4 kPa; nevertheless, results revealed their high sensitivity to saline and high-temperature conditions, where their swelling ratio at 80 °C was 470.4 g/g in deionized water and dropped to 12.61 g/g in

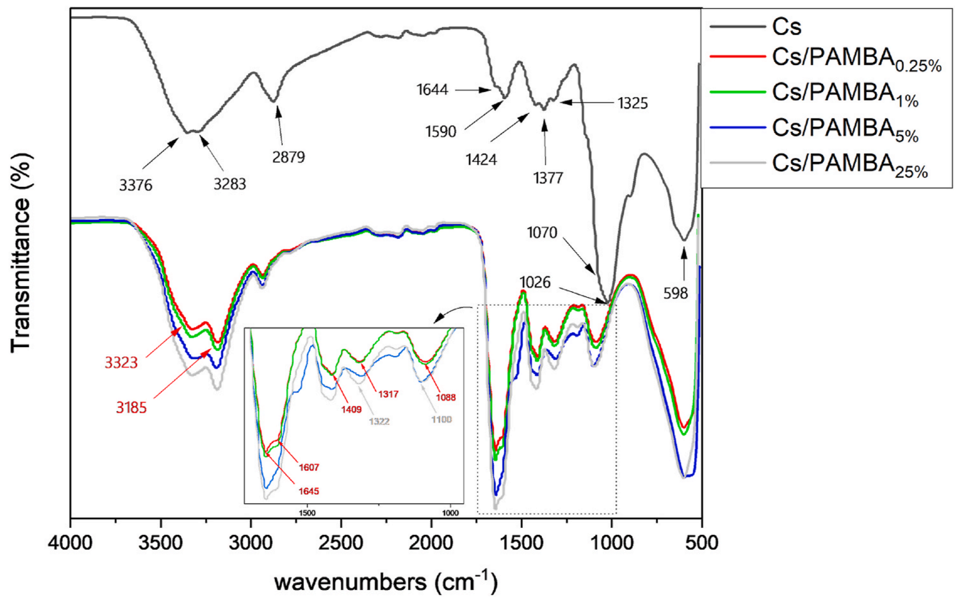

Fig. 3. The FTIR spectra of Cs and Cs/PAMBA at various MBA proportions.

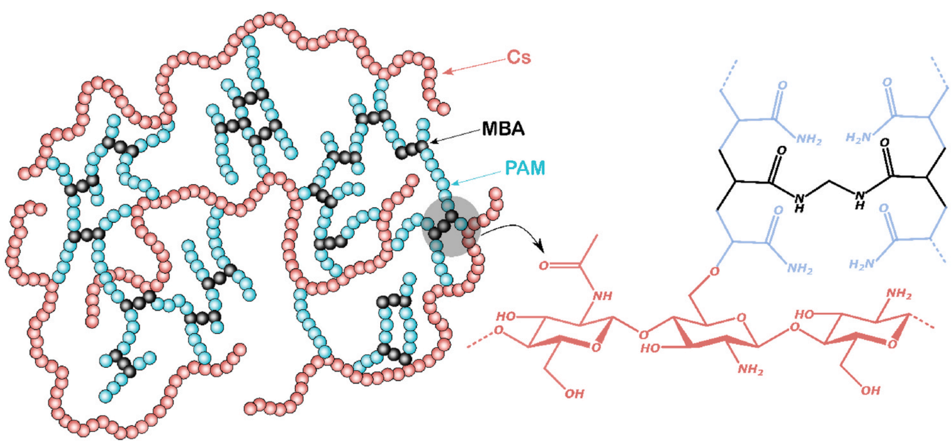

Fig. 4. Proposed structure of Cs/PAMBA.

saline swelling medium of TDS of 149,829 ppm. Additionally, chromium acetate is restricted in the field because it is highly hazardous and harmful to marine life when released, even in small doses (Shamlooh et al., 2020). One investigation has developed PPGs from synthetic chemicals for ultra-high temperature reservoirs, which were tolerable to up to 130 °C with a strength of 640 Pa. Yet, its strength dropped to 184.3 Pa after 3 months (Long et al., 2019). Carbonate reservoirs, such as those found in Gulf countries, are characterized by the extreme salinity of their formation water and the high temperature (over 150 °C), which considerably affect the gel strength and thermal stability of PPGs. Furthermore, the Oslo and Paris Commission (OSPAR) states that the overall effect of offshore chemicals on marine ecology must be minimized. Therefore, developing water control PPGs that are less hazardous, eco-friendly, and can sustain long-term thermal stability for such conditions is crucial.

Polysaccharides (such as chitin and its deacetylated form of chitosan, cellulose, and starch) are an appealing alternative to synthetic polymers due to their biodegradability, non-toxicity, lower cost, and availability. However, polysaccharide applications are challenging due to their low mechanical strength, poor stability, and high degradability, specifically at high temperatures (Kumar et al., 2017). Polysaccharides contain functional groups such as alcohols, carboxylic acids, and amines that are useful for crosslinking or grafting other polymers (Mignon et al., 2019). The grafting of synthetic polymers onto polysaccharide backbones has caught the interest of many researchers, as it is one of the most practical techniques for improving the physicochemical properties of polysaccharides. Grafting is a chemical procedure that modifies some desirable properties in polysaccharide backbones without changing their intrinsic behavior by employing free radical initiation, UV or microwave irradiation, or other methods (Aly and El-Bisi, 2018). The grafting process has been conducted widely in agriculture, water treatment, biomedicine, and other fields (Aly and El-Bisi, 2018). Still, to our knowledge, they have never been used to produce preformed particle gel (PPG) for high-temperature conditions (>90 °C).

Grafted polysaccharides have lately been widely used as superabsorbents or hydrogels due to their capacity to form hydrogen bonds and due to the ionization of their functional groups in water that creates a pressure gradient, inducing the penetration of water into their structures and increasing their size. The application of chitosan-based superabsorbent hydrogels is broadly investigated and applied in various fields (Mahdavinia et al., 2004), (Sohail et al., 2015), (Sabadini et al., 2015), (Cheng et al., 2017), (Bhattacharyya and Ray, 2014). They have been developed using chemical or physical crosslinking methods. Physically crosslinked hydrogels are often linked by hydrogen bonding or

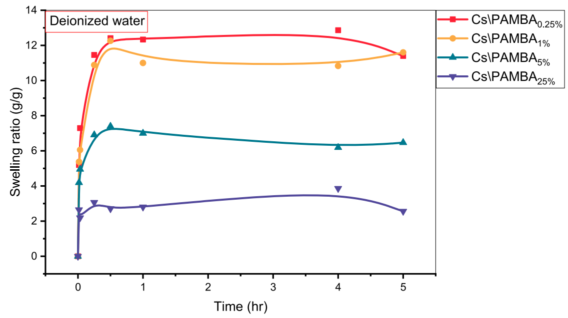

(a)

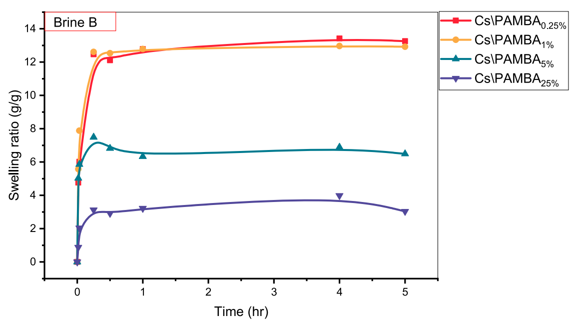

(b)

Fig. 5. Swelling kinetics in different solutions of: (a) Deionized water and (b) Brine B.

electrostatic interactions, creating weak networks, whereas chemically crosslinked hydrogels typically have robust polymeric networks connected by strong covalent bonding (Mignon et al., 2019), (Aly and El-Bisi, 2018), (Cheng et al., 2017).

Chitosan has received much attention in petroleum engineering research since its uses ranged from drilling to oil processing in midstream facilities (Negi et al., 2021). In many review articles, chitosan is also proposed as a green crosslinker for polyacrylamide (PAM) gelation for high-temperature reservoirs for conformance control applications (Negi et al., 2021), (Magzoub et al., 2020), (Hamza et al., 2019), (El-Karsani et al., 2014), (Amir et al., 2019). Despite this, few investigations of in-situ cross-linkable gels have been conducted on the chitosan-based system (Reddy et al., 2003), (George et al., 2017), (Kamarulizam and Ismail, 2020), (Shamlooh et al., 2022). Recently, our group exploited chitosan's good qualities and the superior advantages of PPG and developed a PPG made by physical blending of chitosan and PAM (Elaf et al., 2023). The system showed high swelling capacity and adequate mechanical strength. However, due to its tendency to degrade at higher temperatures, it was recommended for use in reservoirs with moderate temperatures (~75 °C).

Given the literature mentioned above, existing preformed particle gels have faced particular challenges in their application that can be summarized as follow: insufficient temperature resistance, lack of strength and toughness, and rapid degradation at harsh reservoir conditions (Kumar et al., 2020). In addition, there is a need to broaden the scope of green materials in the petroleum field to overcome the market's limited and monopolized synthetic PPGs and save marine ecology. Accordingly, the objective of this research study is to propose a novel, eco-friendly, robust, and thermally stable PPG made of chitosan polysaccharide and polyacrylamide crosslinked with MBA grafted in its backbone (Cs/PAMBA) by microwave irradiation method specified for high temperature (≤130 °C) and high salinity reservoirs (200,000 ppm) for water shutoff. To accomplish this, several samples of Cs/PAMBA with different propotion of MBA were synthesized and analyzed using the infrared spectroscopy analysis method. Thereafter, the effect of MBA weight percent, several operational and reservoir conditions (salinity, pH, temperature), and long-term aging on swelling capacity and mechanical strength were investigated. The morphology of PPGs can shed light on the causes of several observations relating to swelling capacity, rheological characteristics, thermal stability, etc. Thus, thorough scanning electron microscopy (SEM) tests were performed to precisely analyze the swollen PPGs networks in their natural state and under various conditions.

2. Materials and methods

2.1. Chemicals

Chitosan (structure in Fig. 2) with low molecular weight (M_w < 50,000 Da) and 88% degree of deacetylation was obtained from Chito-Lytic, Canada. Acetic acid glacial was acquired from Research Lab, India. Acrylamide (AM, 98%), n, n'-methylenebisacrylamide (MBA, ≥97%), and ammonium persulfate (APS, ≥97.5%) were supplied by Glentham Life Science Ltd, United Kingdom. All the chemicals were used as received without any further purification. All the solutions were prepared in deionized water (DIW).

2.2. Microwave-assisted synthesis of chitosan grafted crosslinked polyacrylamide (Cs/PAMBA)

Different samples of Cs/PAMBA were synthesized with varied weight ratios of MBA crosslinker according to the formulations shown in Table 1. The four materials were synthesized by free radical solution polymerization via grafting of AM/MBA into the Cs backbone, applying a microwave-assisted synthesis technique. The preparation started by separately dissolving 2 g of Cs in 100 mL of 1% acetic acid solution and 0.2 g of APS in 20 mL of deionized water. The two solutions were mixed and placed in a microwave reactor under stirring and irradiation of 600 W. After around 2 min, the irradiation was paused, and a mixture solution of AM/MBA was added to the reaction vessel. After that, the irradiation proceeded again until a gel was produced. If no gelling occurred within 5 min, the irradiation was stopped, and the reaction vessel was left undisturbed to complete the grafting and crosslinking reaction. Afterward, the gel was allowed to cool before being crushed or cut into small pieces and repeatedly washed with deionized water to eliminate undesired chemicals. The grafted material was then collected, dried at 65 °C for 24 h, crushed, and sieved into different particle sizes of 1000–1180 μm, 500–1000 μm, 250–500 μm, 125–250 and ≤ 125 μm.

2.3. Methods

2.3.1. Fourier transform infrared spectroscopy (FTIR)

Fourier transform infrared spectroscopy (FTIR) was performed for dried powders of pure chitosan and Cs/PAMBA using a PerkinElmer Spectrum, KBr disc for direct compression, and 16 scans average at 4.0 cm^{-1} resolution in the wave number range of 400–4000 cm^{-1}. The test was carried out to confirm the grafting copolymerization technique and the chemical structure of the PPGs.

2.3.2. Rheology measurements

Anton Paar MCR 302 rheometer was used to calculate the storage modules (G′) and investigate the linear viscoelastic region (LVR) of the swollen PPGs using the frequency sweeps tests with a range of 0.1–100 Hz and a geometry of parallel plate with a 25 mm diameter and 2 mm spacing. The storage modulus values at 10 Hz were chosen to contrast various gel samples, ensuring that all testing was done in the non-destructive deformation range or inside the LVR at a fixed strain of 10%. The storage modulus (G′), which reflects the gel strength, shows how much stretching or deformation the gel can tolerate before breaking down (Seidy Esfahlan et al., 2021). The PPGs were prepared at predetermined conditions, such as different temperatures, pH, and salinity,

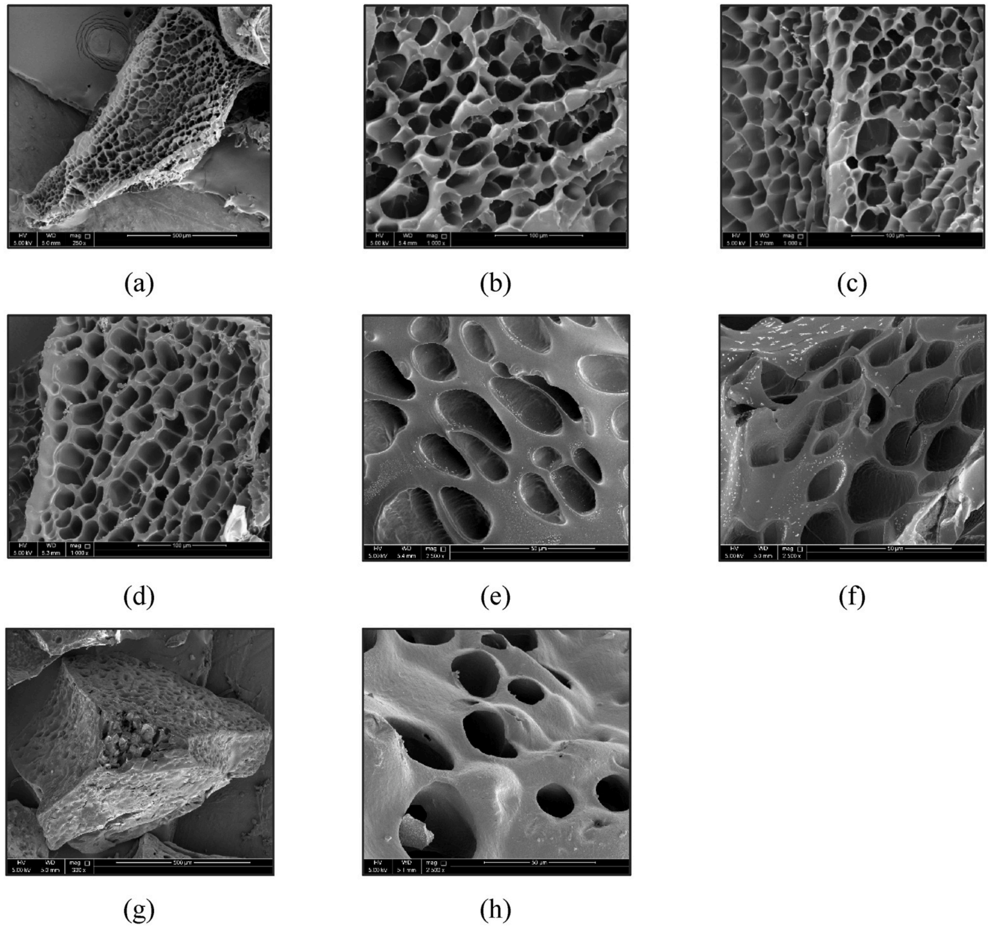

Fig. 6. SEM images for swollen morphology of (a, b, c) Cs/PAMBA$_{0.25\%}$; (d) Cs/PAMBA$_{1\%}$; (e, f) Cs/PAMBA$_{5\%}$; and (g, h) Cs/PAMBA$_{25\%}$ in several magnification levels.

and given enough time to reach their ultimate swelling capacity before performing the rheological testing. Each experiment is repeated twice to guarantee an error of less than 5%.

2.3.3. *Thermo-gravimetric analysis*

The thermal stability of Cs/PAMBA PPG was determined using thermo-gravimetric analysis (TGA) via PerkinElmer Pyris 1 TG A equipment. A sample weight of 2 mg was heated from 30 °C to 700 °C at a rate of 10 °C/min, with a purge of nitrogen flowing at a rate of 35 mL/min.

2.3.4. *Scanning electron microscope (SEM)*

Scanning electron microscopy (SEM) was used to visualize the morphological structures of the dried and swollen PPGs. Before performing the SEM testing, the swollen PPGs were passed through three freeze-drying stages for 48 h using Labconco, FreeZone 12 machine, as the conventional SEM does not accept any humid samples. The drying stages were as follows: (1) the swollen PPGs were frozen at −50 °C at 0.6 °C/min in the freeze-dryer chamber and maintained on an isothermal plateau for 2 h (2) They were sublimated at a temperature of −15 °C and a total gas pressure of 18 Pa. (3) The samples were then dried at a warmer shelf temperature of 25 °C under a pressure of 10 Pa to reduce the residual moisture content to optimum values. The SEM tests were then conducted using FEI Nova Nano SEM 450 microscope, after which the samples were sprayed and coated with gold.

2.3.5. *Swelling ratio measurement*

The swelling ratio was measured using the gravimetric technique, which requires soaking 0.5 g of dry PPGs in 100 mL of distilled water or brine solutions for set periods and predetermined temperature (25–130 °C) or pH (2–12). The considered particle size of the dried PPGs in this study is in the range of 250–500 μm. The PPG samples were left understirring for 24 h to ensure that the solution had contacted all the particles and that they had reached their maximum swelling capacity. The swollen PPGs were separated from the residual solution using filter papers and then weighted to calculate the swelling ratio (g/g) using Equation (1).

$$SR\ (g/g) = \frac{W_s - W_d}{W_d} \tag{1}$$

where W_s is the weight after swelling, and W_d is the weight of dry PPG before swelling.

All the experiments were duplicated to ensure minimal errors, and the average values were considered.

Table 2 illustrates the total dissolved salts (TDS) employed in this study, where pure salts are dissolved in deionized water on the laboratory scale. The specified TDS of the Brine B, which is 67.3 g/L, represents the salinity levels prevalent in oil reserves in Gulf nations (Mahmoud, 2014), (Abdulazeem et al., 2017).

3. Results and discussion

3.1. *FTIR spectroscopy and chemical structure of crosslinked polyacrylamide grafted chitosan*

The FTIR spectra of Cs and the different samples of Cs/PAMBA are displayed in Fig. 3. O–H and N–H groups were observed in a broad band

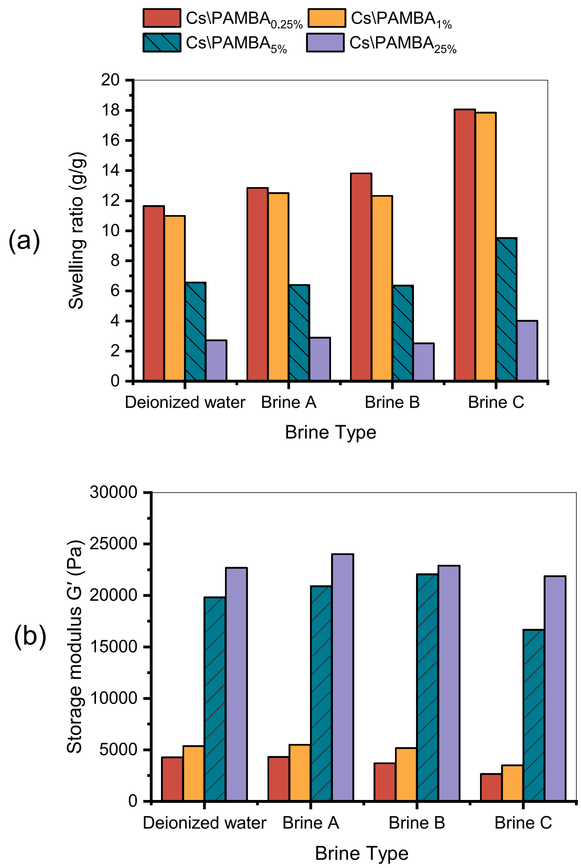

Fig. 7. (a) Swelling ratio (g/g) and (b) Strength of swollen Cs/PAMBA in different salinity media.

in the region 3000–3400 cm^{-1} of the Cs spectrum. The peak at 2879 cm^{-1} was attributed to the stretching of C–H bonds. The bands at 1644 cm^{-1} and 1325 cm^{-1} were due to the stretching of the C=O and C–N functions, respectively. The N–H bending can be seen in 1590 cm^{-1} and the characteristic peaks at 1070 cm^{-1} and 1026 cm^{-1} were due to the C–O stretching and O–H bending, respectively. Some additional bonds, such as CH_2 bending and CH_3 symmetrical deformations, were displayed in the range of 1450 cm^{-1} to 1350 cm^{-1}.

The FTIR spectrum of the Cs/PAMBA indicates that AM and MBA were converted successfully since the C=C strong stretching peak between 995 and 900 cm^{-1} was absent. The grafting of the monomers on the Cs backbone is confirmed by new peaks in the FTIR spectrum of Cs/PAMBA related to crosslinked PAM. The characteristic peaks at 3185 cm^{-1} and 3323 cm^{-1} were attributed to symmetric and asymmetric stretching of the N–H bond in the FTIR spectra of Cs/$PAMBA_{0.25\%}$, vibration bands at 1645 cm^{-1} and 1607 cm^{-1} are attributed to C=O stretching and NH bending, whereas bands at 1409 cm^{-1} and 1317 cm^{-1} are attributed to C–H bending and C–N stretching, respectively. The disappearance of O–H bending at 1026 cm^{-1} proves this group's consumption in the grafted material's structure. In addition, the shifting of the C–O stretching peak from 1070 cm^{-1} to 1088 cm^{-1} in Cs/$PAMBA_{0.25\%}$ proves the formation of a new ether group and confirms the proposed structure in Fig. 4.

Increasing the MBA proportion in Cs/PAMBA raises the intensity of C=O and N–H bands since MBA contains two CONH groups. Furthermore, the new C–O stretching peak in Cs/$PAMBA_{0.25\%}$ at 1088 cm^{-1} and C–N stretching at 1317 cm^{-1} show a maximum increase and shift to 1100 cm^{-1} and 1322 cm^{-1}, respectively, in Cs/$PAMBA_{25\%}$.

3.2. Swelling kinetics

Swelling kinetics describes the evolution of PPG in size as a function of time, establishing how long PPG must remain in the solution to attain its maximum swelling capacity. Based on this time, the optimum placement zone for these PPGs to function as deep plugging or near-wellbore capping will be defined. PPGs are more likely to penetrate deeper in the reservoir the longer it takes them to attain their maximum swelling capacity (Sun et al., 2019). According to Schlumberger, the maximum swelling ratio for PPGs to be effective as deep plugging agents must be reached after 3–5 h, while the maximum swelling capacity for PPGs to be adequate as near-wellbore agents must be at least 1 h. They are considering the mixing time of around 5 min and pumping time of 20–40 min. Some PPGs have different swelling kinetics in different brine solutions and temperature conditions, with faster swelling kinetics recorded for lower-concentration brines and higher temperatures (Salunkhe et al., 2021), (Pu et al., 2019). Therefore, PPGs might be mixed with higher salinity solutions before dumping them into reservoirs to delay the maximum swell capacity and use them as deep plugging agents. The swelling kinetics of several PPGs of Cs/PAMBA in two solutions of deionized water and Brine B (TDS = 67.3 g/L) have been studied, as illustrated in Fig. 5. The swelling ratio profiles were rapid in the first 30 min, then decreased somehow and flattened over the next several hours. Since the Cs/PAMBA PPGs are insensitive to salinity, as discussed in the next section, the swelling kinetics and the swelling ratios in both solutions were the same. After approximately 1 h, the maximum swelling capacity was reached, suggesting them as near-wellbore plugging agents. In addition, the kinetics of the different PPG samples revealed similar trends, suggesting that the MBA amount in the PPG formulations does not affect the swelling time.

3.3. Surface morphology of Cs/PAMBA

A scanning electron microscope (SEM) and ImageJ software were used to characterize the surface structure of the preformed gels and confirm their grafting and crosslinking processes after they had freeze-dried, as shown in Fig. 6. The surface structure of the Cs/$PAMBA_{0.25\%}$ system exhibited many extensively interconnected micro-sized pores with an average diameter of 29 ± 7 μm that form a 3D network resembling a honeycomb, confirming the results of high swelling ratios and high storage modules, as investigated in next section. These pores are thought to be water permeation zones where the hydrophilic groups interact with the water, besides acting as cages for water holding and retention (Lertsarawut et al., 2021). Therefore, the higher number of pores or the larger the pore size, the higher the water content inside the particle gel (Zhou and Wu, 2011). According to Driest et al. a well-defined network structure, which refers to evenly distributed pores of comparable sizes, describes any polymeric system with an ideal or perfect network (Driest et al., 2019). Well-defined network structures may equally distribute stresses across the polymer matrix, enhancing the PPG's mechanical properties (Zhou and Wu, 2011). Based on the SEM images, Cs/PAMBAs exhibited well-defined microscopic network structures, which justifies their high strength and hydrolytically and thermally durable characteristics, as shown in the coming sections.

Moreover, when comparing Fig. 6c with Fig. 6d, which represent Cs/$PAMBA_{0.25\%}$ and Cs/$PAMBA_{1\%}$, respectively, one can notice that both PPGs have similar pore sizes and distribution, which provide them with almost the same swelling ratios of 11.64 and 11.00 g/g, respectively. In contrast, Cs/$PAMBA_{5\%}$ (Fig. 6f) has a lower swelling ratio of 6.57 g/g, mainly attributed to fewer pores and smaller pores' sizes with an average of 18 ± 5 μm. The least swelling ratio of 2.72 g/g can be found in Cs/$PAMBA_{25\%}$, which has a limited number of pores, as shown in Fig. 6h. Accordingly, the type of porosity matrix here is determined by the amount of crosslinker (MBA), where the highest content in PPG formulation, such as in Cs/$PAMBA_{25\%}$, has the least number of pores and swellability. Chavda and Patel (2011) have investigated the effect of

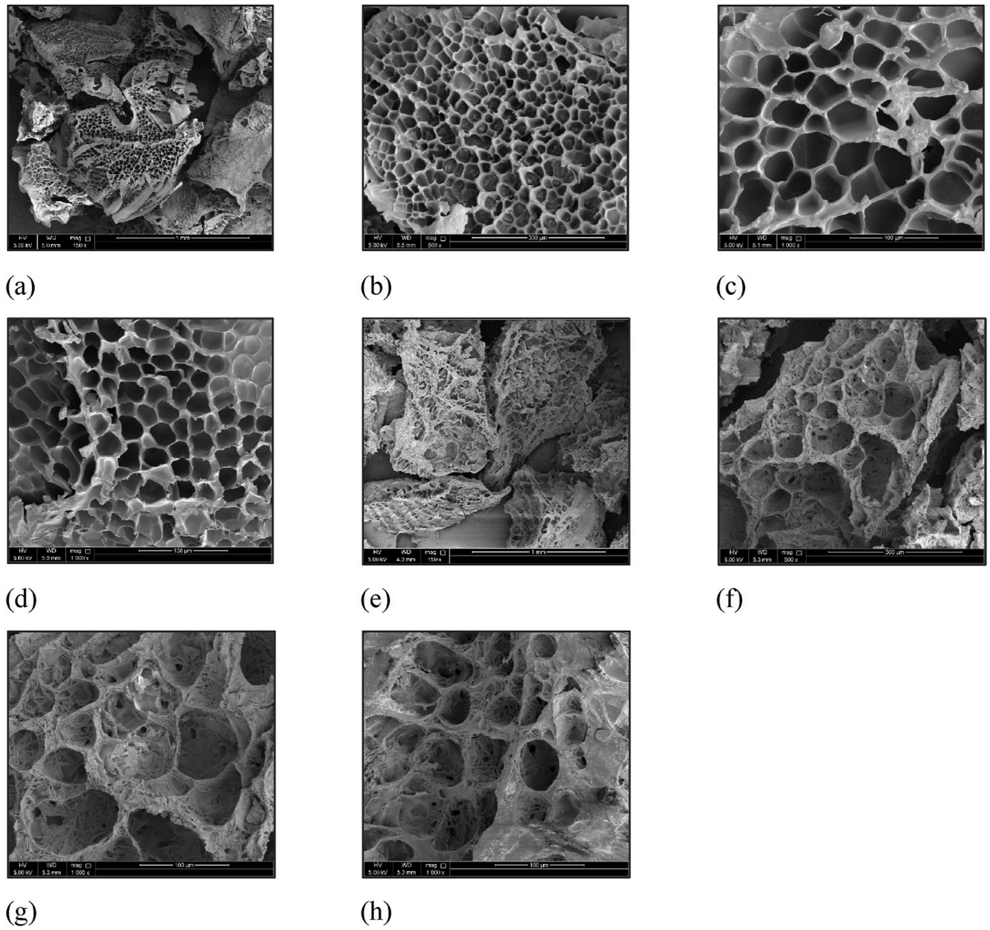

Fig. 8. SEM images of swelled Cs/PAMBA$_{1\%}$ for 24 h at different swelling medium of: (a, b, c, d) DIW, and (e, f, g, h) Brine B in different magnification levels of 150x, 500x, and 1000x.

MBA crosslinker amount on the porosity of the hydrogels and found similar results, where higher crosslinking density leads to diminishing the porosity spaces and thus lower swelling capacities (Chavda and Patel, 2011).

3.4. Factors affecting PPG performance

3.4.1. Salinity factor

Preformed particle gels (PPGs) are thought to be stable throughout a range of reservoir mineralogies, yet, certain PPGs showed pronounced changes in their swelling ratio and gel strength (Heidari et al., 2019b). Therefore, estimating the behavior of the developed PPGs in different salinity media is crucial. Four PPGs of Cs/PAMBA with varying proportions of crosslinker were dispersed into deionized water, Brine A, Brine B (TDS = 67.2976 g/L), and Brine C (TDS = 200 g/L), as shown in Fig. 7a.

The swelling capacities of Cs/PAMBA PPGs showed a slight increase with increasing salinity in DIW, Brine A, and Brine B. In contrast, they have risen remarkably in Brine C by 2–5 g/g relative to other brines. For instance, the swelling capacity of Cs/PAMBA$_{0.25\%}$ was 11.64 g/g in DIW, 12.86 in Brine A, and 13.82 g/g in Brine B, and increased to 18.06 g/g in Brine C. According to the literature, conventional PPGs exhibit the opposite behavior in saline environments than Cs/PAMBA PPGs, where the swelling ratio decreases as the salinity concentration rises. This is may due to an osmotic pressure gradient between the interior of the gel particles and the swelling medium, which causes the solution to permeate into the PPG network (Bai et al., 2007).

Saber-Samandari et al. have developed a semi-interpenetrating polymer network hydrogel of chitosan-g-polyacrylamide and studied the swelling capacity to be reduced by the increase in salt concentration (Saber-Samandari et al., 2012a). Kim et al. found a similar finding in the case of hydrogels made of chitosan and poly (hydroxyethyl methacrylate) (Kim et al., 2005). Therefore, one can conclude that our developed PPGs of Cs/PAMBA are insensitive to salinity, where the addition of salts does not influence their structures and swelling ratios. The rigid and dense 3D network structures of the developed chitosan grafted cross-linked polyacrylamide with MBA create steric hindrance that limits their capacity to undergo shrinking or collapse in the presence of ions, overcoming the interaction forces. Lenji et al. suggested that the rigidity of PPG structures restricts the expansion of gel particles and the capacity of water to enter the network (Lenji et al., 2018b). However, this behavior could be up to a certain salinity level, where at a higher brine solution of a TDS of 200 g/L, the swelling ratios have increased. A proposed justification could be due to the increased amount of ions/salts that enter the gel structure, creating a higher concentration inside the gel particles compared to the swelling medium. Thus, it enhances water entry from the swelling medium into the particle gels and slightly increases the swelling ratios. A parallel discovery was found in a re-crosslinkable polymeric hydrogel in ionic environments where the swelling capacity increases with higher brine salinity, which has been justified by the reduction in the entanglement of the ionic polymer chains disrupted by salts (Wang et al., 2017).

Fig. 7b illustrates the gel strengths of four developed Cs/PAMBA PPGs and confirms the above-proposed mechanism. Since swelling capacity and gel strength have an inverse relationship, and as the developed Cs/PAMBA PPGs suggested to be insensitive to salinity with

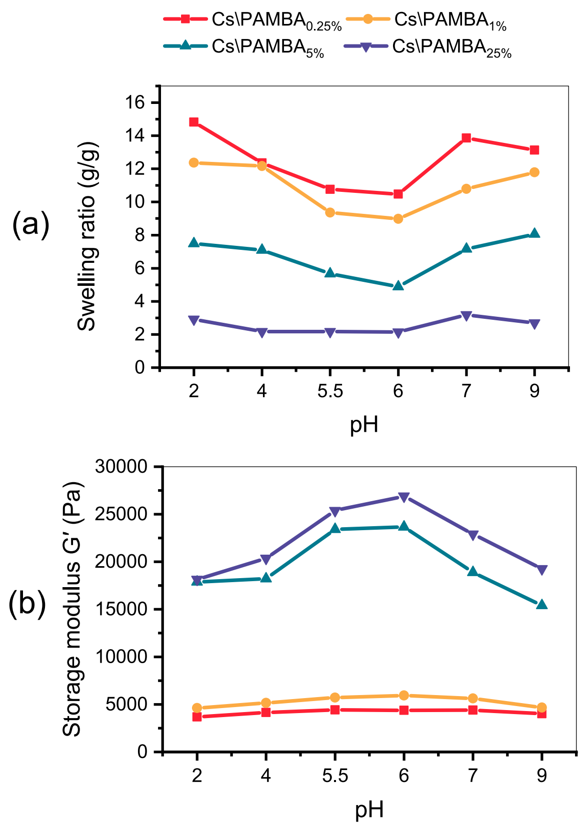

Fig. 9. The effect of pH on the (a) swelling ratio (g/g) and (b) storage modulus (G′) of swollen Cs/PAMBA in Brine B for 24 h.

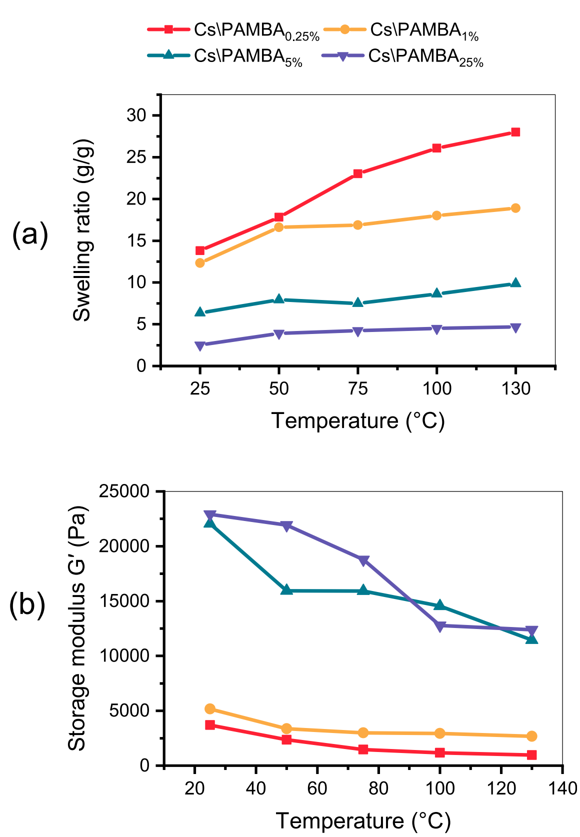

Fig. 10. The (a) swelling ratio and (b) storage modulus (G′) of Cs/PAMBA in the temperature range (25–130 °C) in Brine B for 24 h.

approximately the same swelling ratios, their gel strengths were almost similar in deionized water, and the other two brines of A and B. In contrast, increased swelling ratios in the case of Brine C (200,000 ppm) have reduced the gel strengths. For instance, the storage modulus for Cs/PAMBA$_{0.25\%}$ was 4272.10, 4304.30, and 3699.60 Pa in deionized water, Brine A, and Brine B, respectively, and reduced to 2647.70 Pa in Brine C.

Several SEM images were obtained to understand more about the behavior of Cs/PAMBA in the saline swelling medium (Fig. 8). One can notice that the pores in the particle gels were almost smooth in DIW compared to those in Brine B, which showed a rough surface due to the accumulation of ions. Moreover, when analyzing the pores sizes on both surfaces using ImageJ, the size of the pores in brine was larger than those in DIW, with an average of 24 ± 12 μm and 34 ± 22 μm, respectively. This fact was aligned with the above-proposed justification, as the larger the pore size, the more water entry, and the higher swelling ratios. Furthermore, an interesting observation of extensive and tiny networks when zooming on the surface of Cs/PAMBA$_{1\%}$ swelled in Brine B (Fig. 8h). These tiny networks may also act as cages for water retention, contributing to a higher swelling ratio. The small networks result from physical crosslinking between the COO^- and NH_3^+ groups in the gel chains and the multivalent ions in Brine B, such as Mg^{2+}, Ca^{2+}, CO_3^{2-}, etc.

3.4.2. PH factor

Some reservoirs have large amounts of highly acidic components, such as carbonate reservoirs, which may interact with the injected PPGs, changing their qualities and behavior (Abdulbaki et al., 2014). Therefore, this part of the investigation examines the sensitivity of PPGs to pH by including various swelling mediums of Brine B that were adjusted by adding diluted NaOH and HCl droplets. Fig. 9a illustrates how the pH variation has altered swelling ratios of the developed Cs/PAMBA PPGs after 24 h at 25 °C. The swelling ratios were lowest at pH 6.0 and maximum in the acidic and basic media at pH 2.0–4.0 and pH 7.0–9.0, respectively. The protonated amine groups into ammonium cations ($-NH_3^+$) in the chitosan are responsible for such behavior in the acidic medium because they induce electrostatic repulsions that raise the charge density inside the gels' networks, causing water to penetrate the gels and thus improve their swelling ratios. Increasing the pH up to 6 will result in the deprotonation of amine groups in chitosan, which in turn reduces the charge density and swelling ratios. Similar findings were found in the following chitosan-based studies (Saber-Samandari et al., 2012a), (Saber-Samandari et al., 2012b), (Budianto and Amalia, 2020). In the basic medium, the electrostatic repulsions of the carboxylate groups ($-COO^-$), which are produced by basic hydrolysis of amide groups, comes into action to increase the charge density and, thus the osmotic pressure and water absorbency (Rani et al., 2018).

Fig. 9b shows the storage modules (G') of Cs/PAMBA PPGs in different pH-adjusted solutions. The results were aligned with the swelling ratios, where the highest water absorbency has the lowest gel strength and vice versa. For example, Cs/PAMBA$_{0.25\%}$ has a swelling ratio and storage modulus of 14.83 g/g and 3688.3 Pa at pH 2, 10.47 g/g and 4369.3 Pa at pH 6, and 13.13 g/g and 4027.5 Pa at pH 9. Overall, Cs/PAMBA did not exhibit any deterioration in their bonds and maintained their high storage modulus when swelled in various pH mediums. Thus, they are insensitive to pH fluctuations and practical in different reservoir environments, including highly acidic ones.

3.4.3. Temperature factor

As many reservoirs may reach temperatures of up to 150 °C (El-Karsani et al., 2014), it is critical to consider the temperature factor while developing a PPG system to ensure sufficient durability and thermal stability. Thus, known weights of Cs/PAMBAs were soaked in Brine B, sealed in screw-cap bottles, and immersed in an oil bath for 24 h of heating at predetermined temperatures of 50, 75, 100, and 130 °C. Fig. 10a illustrates the swelling capacities of the Cs/PAMBAs relative to temperature variation. Results showed that the water absorbency of

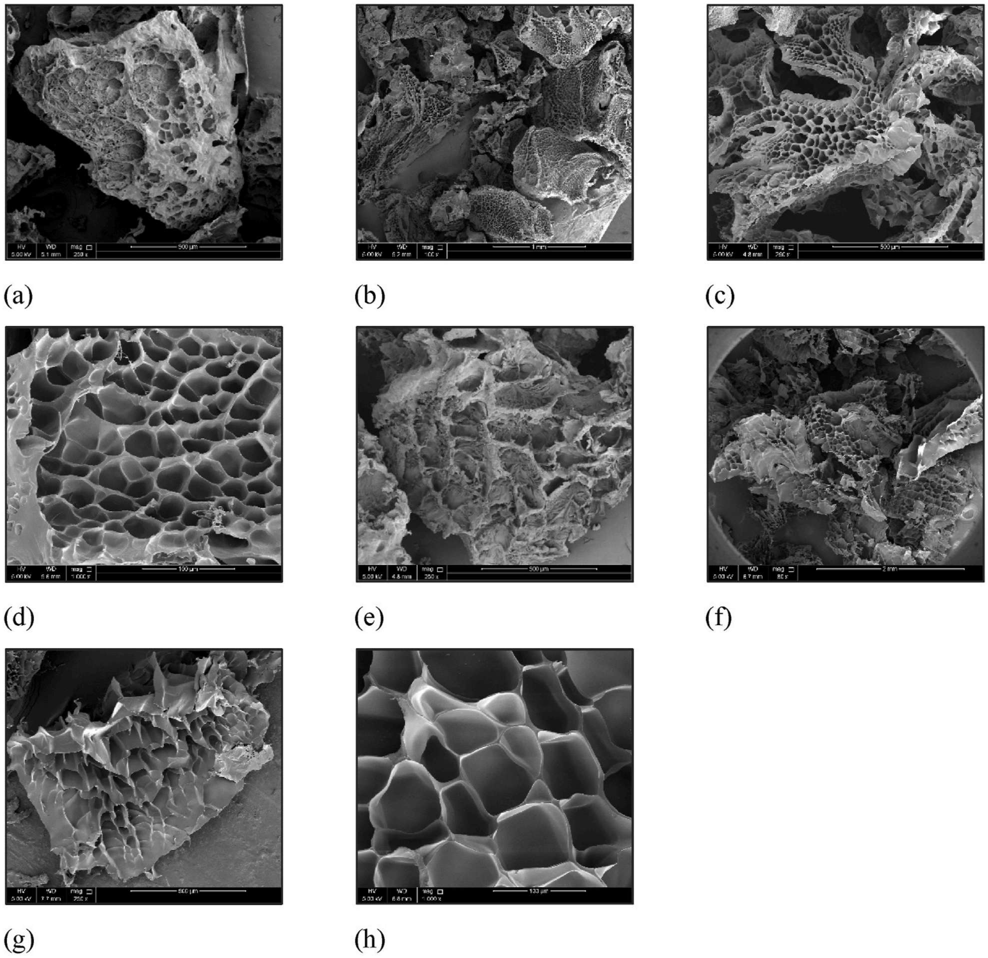

Fig. 11. SEM images of swelled Cs/PAMBA$_{0.25\%}$ for 24 h at different temperatures of (a, b, c, d) 25 °C, and (e, f, g, h) 100 °C in different magnification levels of (f) 80x, (b) 100x, (a, e, c, g) 250x, and (d, h) 1000x.

Cs/PAMBAs increased by increasing the temperature. This behavior is properly related to the expansion of PPG's structure and to the formation of the carboxyl group (–COOH) produced as a result of the thermal hydrolysis of amide groups (–$CONH_2$) (Bai et al., 2007). Carboxyl groups are strong hydrophilic groups that increase water uptake, raising the swelling ratios. In addition, it was noticed that the PPG with the least amount of crosslinker, such as Cs/PAMBA$_{0.25\%}$, was impacted most in thermal conditions, as its swelling ratio was duplicated at 130 °C compared to 25 °C. In contrast, the swelling ratio of Cs/PAMBA$_{25\%}$ was slightly increased due to its rigid, dense structure.

The elasticity behavior of the PPGs was also examined, as shown in Fig. 10b. The gel strengths decreased with the thermal factor, which is related to the increased water uptake. The storage modules of Cs/PAMBA$_{0.25\%}$, Cs/PAMBA$_{1\%}$, Cs/PAMBA$_{5\%}$, and Cs/PAMBA$_{25\%}$ were 3699.6, 5176.6, 22057, and 22910 Pa, respectively, at 25 °C while decreased to 976, 2674, 11454, and 12388 Pa, respectively, at 130 °C. One can conclude that all Cs/PAMBAs exhibited excellent thermal behavior as there is no sense of any structure deterioration or degradation even with the highest temperature of 130 °C. In addition, their storage modules were still high and adequate to resist the stresses in the high-temperature reservoirs.

The SEM images in Fig. 11 can validate the justification mentioned above. One can notice that the PPG structure undergoes expansion with the temperature factor, where the pores become larger in size, allowing more water to diffuse into the polymeric matrix, thus, a higher swelling capacity. Based on ImageJ software, the average pore size of Cs/PAMBA$_{0.25\%}$ at room temperature and in Brine B (Fig. 11a) was 51 ± 14 μm, while expanded to 106 ± 48 μm at 100 °C in Brine B (Fig. 11e). This expansion was the reason for the enhanced swelling ratio from 13.82 to 26.09 g/g when the temperature increased from 25 to 100 °C, as seen in Fig. 10a. In addition, comparing Fig. 11d with Fig. 11h, having the same magnification of 1000x, the average pore size of Cs/PAMBA$_{0.25\%}$ after swollen in distilled water was 29 ± 7 μm at 25 °C and increased to 58 ± 22 μm at 100 °C.

3.5. Long-term thermal stability

The most challenging aspects when designing a preformed particle gel treatment system are its ability to stay durable in reservoirs of harsh conditions and its long-term thermal stability (Tongwa and Bai, 2014). This part of study included both effects of high temperature and high salinity besides the time factor to test the thermal and hydrolytic behavior of Cs/PAMBA PPGs in the long term. The PPGs of Cs/PAMBA$_{0.25\%}$, Cs/PAMBA$_{1\%}$, Cs/PAMBA$_{5\%}$, and Cs/PAMBA$_{25\%}$ were thus weighted and dispersed in Brine B in sealed bottles and submersed in an oil bath with a fixed temperature of 100 °C for 1 day, 15 days, and 30 days. The key considerations in this investigation are the swelling ratios and mechanical strengths. The reduction of gel strength could be because of several reasons. First, due to an expected increase in the swelling ratio resulting from high temperature. Second, due to degradation rates, where in this case, the swelling ratio is also reduced. As illustrated in Fig. 12a, the swelling ratios of all PPGs after 15 days aging have either remained almost the same, as in the case of Cs/PAMBA$_{0.25\%}$, or have increased slightly by 15%, like Cs/PAMBA$_{1\%}$, or increased

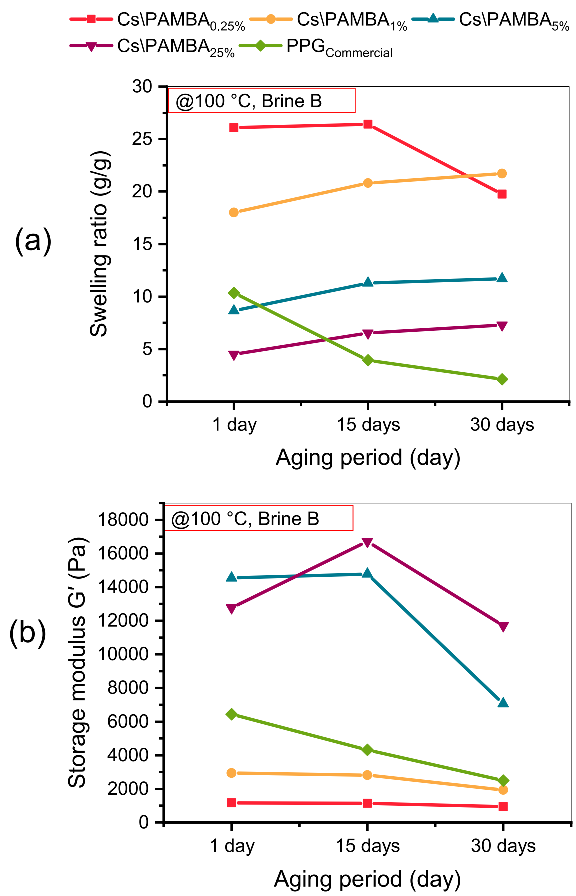

Fig. 12. Aging effect on the (A) swelling ratio and (B) strength of Cs/PAMBA PPGs and a commercial PPG at 100 °C in Brine B.

significantly, as in the case of Cs/$PAMBA_{5\%}$, and Cs/$PAMBA_{25\%}$. Modest decreases in the gel strengths followed these increased swelling ratios after 15 days (Fig. 12b), which are reasonable and do not remark any degradation traces in the PPGs' structures. After one month, the swelling ratios of Cs/$PAMBA_{1\%}$ and Cs/$PAMBA_{5\%}$ were further increased by an average of 4%, while Cs/$PAMBA_{25\%}$ increased by 12% compared to day 15.

In contrast, Cs/$PAMBA_{0.25\%}$ exhibited a decrease in its swelling ratio by −25% relative to day 15, followed by decrease in its mechanical strength from 1141.3 Pa to 942.4 Pa. Overall, PPGs of chitosan grafted polyacrylamide with 1–25 wt% of MBA exhibited outstanding behaviors, where the swelling ratios were 7.3–22 g/g and the gel strengths were in the range of 1935.5–11704 Pa after 1 month of ageing in harsh conditions. It is worth noting that a higher amount of MBA (crosslinker) was directly proportional to long-term thermal stability, where the structure becomes more durable and thermally resistant. Tongwa and Bai (2014) have shown that adding higher nanomaterial concentrations improves PPG's long-term thermal stability (Tongwa and Bai, 2014).

Furthermore, one can notice that the commercial PPG (green line) was thermally degraded after 15 days, as its swelling ratio decreased by −62%, followed by a significant drop in its gel strength by −33%, rendering it thermally unstable in the long run. Bai et al. stated that PPG is thermally stable when it retains 80% of its original strength at a specific temperature (Bai et al., 2007).

As illustrated in Fig. 13, the chitosan-grafted polyacrylamide PPGs maintained their structures after 15 days of aging, as indicated by SEM images. Fig. 13c demonstrates the robustness of the structure with smaller pore sizes coupled heavily in a vast 3D network, whereas Fig. 13a displays a brittle network with larger pore sizes that may be destroyed with further heating. Therefore, the MBA role as a crosslinker was revealed, where the higher its concentration in the formulation, the more rigid and thermal durable structure of PPG produced.

Thermogravimetric analysis (TGA) is another method for examining the PPGs' thermal stability. TGA was applied for pure chitosan and other grafted materials of Cs/PAMBA with a heating temperature range of 25–700 °C, as presented in Fig. 14. Two distinct regions of considerable weight loss have been noted for chitosan, and three regions for Cs/PAMBA, as shown in Fig. 14b. For the chitosan, the first thermally degraded zone, accounting for less than 10% weight loss, occurs in the temperature range of 30–100 °C, attributed to the evaporation of the residual moisture content. The second thermal incident occurs between 240 and 400 °C, accounting for 45% of weight loss, which is related to the decomposition of the functional groups (Ma et al., 2016). In comparison, grafting crosslinked PAM to the chitosan has increased the thermal stability and endurance, where the three grafted materials exhibited a slight weight loss of approximately 30% at 225–340 °C; and the significant degradation region of about 40% weight loss started from 360 to 460 °C, attributed to the crosslinked PAM degradation. Thus, these findings suggest that the copolymerization of Cs/PAMBA produced thermally stable structures that maintained 80% of their original weight at a temperature of 290 °C, which is more than the region of interest of high-temperature reservoirs (150 °C).

4. Conclusion

An eco-friendly preformed particle gel (PPG) was created chemically using a microwave irradiation process and APS as an initiator to graft several ratios of AM/MBA onto the backbone of the polysaccharide chitosan. Many methods are used to characterize the developed grafted material of Cs/PAMBA and to test its performance under diverse reservoir conditions in the short and long run, including the FTIR, SEM, Rheology, and swelling measurements. The study successfully integrated the chitosan polysaccharide with synthetic polymers to create greener PPG with superior properties to those found in currently available PPGs, including long-term thermal stability, high strength, and adequate swelling capacities under the harsh conditions of reservoirs. The key findings from this study are as follows.

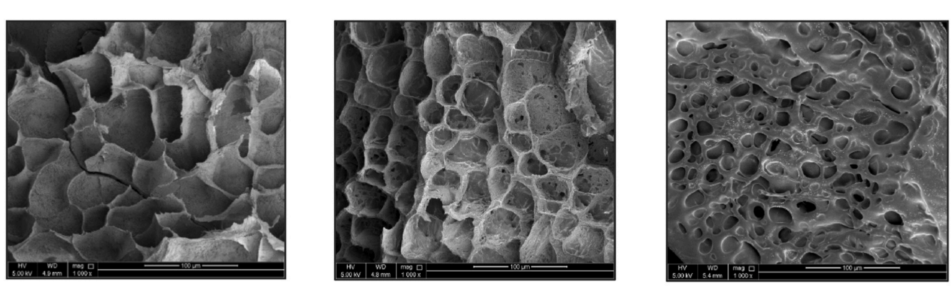

(a) (b) (c)

Fig. 13. SEM images at magnification 1000x of (a) Cs/$PAMBA_{0.25\%}$, (b) Cs/$PAMBA_{1\%}$, and (c) Cs/$PAMBA_{5\%}$ after aging at 100 °C in brine 2 for 15 days.

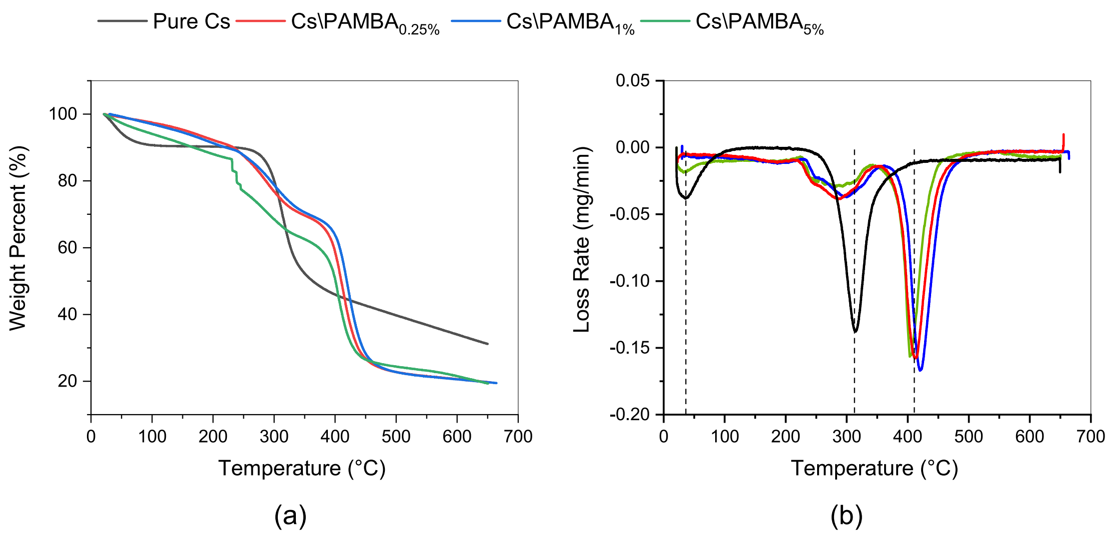

Fig. 14. Thermogravimetric analysis for pure chitosan and chitosan-grafted polyacrylamide, (a) Weight Percent (b) Loss Rate.

- FTIR analysis has demonstrated the grafting reaction between the chitosan and crosslinked polyacrylamide, which is observed by the interaction of hydroxyl groups in chitosan and the vinyl groups in acrylamide. Besides, the SEM images visually confirmed the cross-linking and showed 3D network structures with interconnected micro-sized pores with an average diameter of 29 ± 7 μm for Cs/PAMBA$_{0.25\%}$.
- The Cs/PAMBA PPGs have fast swelling kinetics in both deionized water and Brine B, where the maximum swelling capacities have reached after 1 h, suggesting them as near-wellbore plugging agents.
- The swelling ratios in deionized water were between 2.71 and 11.64 g/g, while 2.52–13.82 g/g in Brine B (TDS = 67.3 g/L), and increased to 4.01–18.06 g/g in a Brine C (TDS = 200 g/L). The storage modules were 4272–22687 Pa in deionized water, 3699.6–22910 Pa in Brine B, and 2647.7–21876 Pa in Brine C, depending on the MBA content in the PPG formulation. Therefore, the Cs/PAMBA PPGs are insensitive to salinity with a TDS of up to 67.3 g/L and increased slightly to 200 g/L due to osmotic pressure difference.
- The alkalinity and acidity conditions and the high temperatures stimulate the swelling ratios but slightly decrease the mechanical strengths of the gels, mainly related to the functional groups' hydrolysis in such conditions and electrostatic repulsions.
- Tests confirmed the ability of Cs/PAMBA PPGs to withstand temperatures of up to 130 °C. In addition, the system showed long-term thermal stability at 100 °C & high salinity, indicating that it might be a good system for commercialization and utilization in reservoirs with high temperatures and salinity.
- This study recommends future work on core flooding and filtration tests using real carbonate core samples to accurately evaluate the sealing ability and plugging efficiency of developed Cs/PAMBA gels.

Declaration of competing interest

The authors declare that they have no known competing financial interests or personal relationships that could have appeared to influence the work reported in this paper.

Data availability

Data will be made available on request.

Acknowledgment

The authors would like to acknowledge the Qatar National Research Fund (a member of Qatar Foundation) for funding through Grant # NPRP13S-1231-190009. Al-Salam Petroleum Services Company inQatar is also acknowledged for co-funding this project. The findings achieved herein are solely the responsibility of the authors. The authors would like to acknowledge Qatar University for providing Graduate Assistantship to Ms. Reem Elaf in her graduate studies. The SEM images were accomplished in the Central Laboratories unit at Qatar University, and the authors would also like to thank them for their continued assistance.

References

Abdulazeem, A., Mahmoud, M., Elkatatny, S., Barri, A., Muhammadain, A., 2017. Development of new seawater-based formulation to stimulate sandstone formations. Soc. Pet. Eng. - SPE Kingdom Saudi Arab. Annu. Tech. Symp. Exhib. 460–468. https://doi.org/10.2118/188004-ms, 2017.

Abdulbaki, M., Huh, C., Sepehrnoori, K., Delshad, M., Varavei, A., 2014. A critical review on use of polymer microgels for conformance control purposes. J. Pet. Sci. Eng. 122, 741–753. https://doi.org/10.1016/j.petrol.2014.06.034. Oct.

Aly, A.A., El-Bisi, M.K., 2018. Grafting of polysaccharides: recent advances. In: Biopolymer Grafting: Synthesis and Properties. Elsevier Inc., pp. 469–519. https://doi.org/10.1016/B978-0-323-48104-5.00011-1

Amir, Z., Said, I.M., Jan, B.M., 2019. In situ organically cross-linked polymer gel for high-temperature reservoir conformance control: a review. Polym. Adv. Technol. 30 (1), 13–39. https://doi.org/10.1002/pat.4455. Jan.

Aqcheli, F., Salehi, M.B., Pahlevani, H., Taghikhani, V., 2020. Rheological properties and the micromodel investigation of nanosilica gel-reinforced preformed particle gels developed for improved oil recovery. J. Pet. Sci. Eng. 192, 107258 https://doi.org/10.1016/j.petrol.2020.107258. Sep.

Bai, B., Li, L., Liu, Y., Liu, H., Wang, Z., You, C., 2007. Preformed Particle Gel for Conformance Control: Factors Affecting its Properties and Applications. https://doi.org/10.2118/89389-pa.

Baloochestanzadeh, S., Hassanajili, S., Escrochi, M., 2021. Rheological properties and swelling behavior of nanocomposite preformed particle gels based on starch-graft-polyacrylamide loaded with nanosilica. Rheol. Acta 60 (10), 571–585. https://doi.org/10.1007/s00397-021-01287-z. Oct.

Bhattacharyya, R., Ray, S.K., 2014. Micro- and nano-sized bentonite filled composite superabsorbents of chitosan and acrylic copolymer for removal of synthetic dyes from water. Appl. Clay Sci. 101, 510–520. https://doi.org/10.1016/j.clay.2014.09.015. Nov.

Budianto, E., Amalia, A., 2020. Swelling behavior and mechanical properties of Chitosan-Poly(N-vinyl-pyrrolidone) hydrogels. J. Polym. Eng. 40 (7), 551–560. https://doi.org/10.1515/polyeng-2019-0169. Aug.

Chavda, H., Patel, C., 2011. Effect of crosslinker concentration on characteristics of superporous hydrogel. Int. J. Pharm. Investig. 1 (1), 17. https://doi.org/10.4103/2230-973x.76724.

Cheng, B., Pei, B., Wang, Z., Hu, Q., 2017. Advances in chitosan-based superabsorbent hydrogels. RSC Adv. 7 (67), 42036–42046. https://doi.org/10.1039/C7RA07104C.

Cheng, L., et al., 2022. Experimental investigation of a novel nanocomposite particle gel for water shutoff treatment in mature oilfields. ACS Omega 7 (10), 8887–8895. https://doi.org/10.1021/acsomega.1c07242. Mar.

Driest, P.J., Dijkstra, D.J., Stamatialis, D., Grijpma, D.W., 2019. The trimerization of isocyanate-functionalized prepolymers: an effective method for synthesizing well-defined polymer networks. Macromol. Rapid Commun. 40 (9), 1800867 https://doi.org/10.1002/marc.201800867. May.

Elaf, R., Ben Ali, A., Saad, M., Hussein, I.A., Nimir, H., Bai, B., 2023. Biodegradable preformed particle gel (PPG) made of natural chitosan material for water shut-off application. Polymers (Basel) 15 (8). https://doi.org/10.3390/polym15081961, 1961.

El-Karsani, K.S.M., Al-Muntasheri, G.A., Hussein, I.A., 2014. Polymer systems for water shutoff and profile modification: a review over the last decade. SPE J. https://doi.org/10.2118/163100-PA.

Farasat, A., Vafaie Sefti, M., Sadeghnejad, S., Saghafi, H.R., 2017. Mechanical entrapment analysis of enhanced preformed particle gels (PPGs) in mature reservoirs. J. Pet. Sci. Eng. https://doi.org/10.1016/j.petrol.2017.07.028.

Farasat, A., Younesian-Farid, H., Sadeghnejad, S., 2021. Conformance control study of preformed particle gels (PPGs) in mature waterflooded reservoirs: numerical and experimental investigations. J. Pet. Sci. Eng. 203, 108575 https://doi.org/10.1016/j.petrol.2021.108575. October 2020.

George, S.C., Patil, P.R., Das, P., 2017. Crosslinking chitosan for reducing permeability in a well. U.S. Patent 611 (9), 420.

Hamza, A., Shamlooh, M., Hussein, I.A., Nasser, M., Salehi, S., 2019. Polymeric formulations used for loss circulation materials and wellbore strengthening applications in oil and gas wells: a review. J. Pet. Sci. Eng. 180, 197–214. https://doi.org/10.1016/j.petrol.2019.05.022. Sep.

Heidari, S., et al., 2019a. Determination of swelling behavior and mechanical and thermal resistance of acrylamide–acrylic acid copolymers under high pressures and temperatures. Iran. Polym. J. 28 (12), 1001–1013. https://doi.org/10.1021/acsomega.1c02638.

Heidari, A., Vasheghani-Farahani, E., Vafaie-Sefti, M., 2019b. Preformed particle gels of sulfonated polyacrylamide: preparation, characterization, and application as permeability modifier. Iran. Polym. J. 28 (12), 1001–1013. https://doi.org/10.1007/s13726-019-00759-7.

Heidari, S., Mohammadi, M., Esmaeilzadeh, F., Mowla, D., 2021. Determination of swelling behavior and mechanical and thermal resistance of acrylamide–acrylic acid copolymers under high pressures and temperatures. ACS Omega 6 (37), 23862–23872. https://doi.org/10.1021/acsomega.1c02638. Sep.

Kamarulizam, S., Ismail, S., 2020. Investigation on guar gum and chitosan based polymer composite for oilfield water shut off fluid. Int. J. Agric. Appl. Sci. 1 (1), 6–13. https://doi.org/10.52804/ijaas2020.112. Jun.

Kim, S.J., Shin, S.R., Shin, D.I., Kim, I.Y., Kim, S.I., 2005. Synthesis and characteristics of semi-interpenetrating polymer network hydrogels based on chitosan and poly (hydroxy ethyl methacrylate). J. Appl. Polym. Sci. 96 (1), 86–92. https://doi.org/10.1002/app.21407. Apr.

Kumar, D., Pandey, J., Raj, V., Kumar, P., 2017. A review on the modification of polysaccharide through graft copolymerization for various potential applications. Open Med. Chem. J. 11 (1), 109–126. https://doi.org/10.2174/1874104501711010109. Sep.

Kumar, A., Mahto, V., Sharma, V.P., 2020. Reinforced preformed particle gel: synthesis, characterization and performance evaluation for water shut-off jobs in heterogeneous reservoir. J. Pet. Sci. Eng. 193, 107408 https://doi.org/10.1016/j.petrol.2020.107408. Oct.

Lenji, M.A., Haghshenasfard, M., Sefti, M.V., Salehi, M.B., Heidari, A., 2018. Experimental study of swelling and rheological behavior of preformed particle gel used in water shutoff treatment. J. Pet. Sci. Eng. 169, 739–747. https://doi.org/10.1016/j.petrol.2018.06.029.

Lertsarawut, P., et al., 2021. Starch-based super water absorbent: a promising and sustainable way to increase survival rate of trees planted in arid areas. Polymers (Basel) 13 (8). https://doi.org/10.3390/polym13081314.

Long, Y., Yu, B., Zhu, C., 2019. Conformance improvement for ultra-high-temperature reservoir: a comparative study between hydrostable and conventional preformed particle gel. In: Society of Petroleum Engineers - Abu Dhabi International Petroleum Exhibition and Conference 2018. ADIPEC, pp. 1–10. https://doi.org/10.2118/192738-ms, 2018.

Ma, J., Fu, K., Shi, J., Sun, Y., Zhang, X., Ding, L., 2016. Ultraviolet-assisted synthesis of polyacrylamide-grafted chitosan nanoparticles and flocculation performance. Carbohydr. Polym. 151, 565–575. https://doi.org/10.1016/j.carbpol.2016.06.002. Oct.

Magzoub, M.I., Salehi, S., Hussein, I.A., Nasser, M.S., 2020. Loss circulation in drilling and well construction: the significance of applications of crosslinked polymers in wellbore strengthening: a review. J. Pet. Sci. Eng. 185, 106653 https://doi.org/10.1016/j.petrol.2019.106653. Feb.

Mahdavinia, G., Pourjavadi, A., Hosseinzadeh, H., Zohuriaan, M., 2004. Modified chitosan 4. Superabsorbent hydrogels from poly(acrylic acid-co-acrylamide) grafted chitosan with salt- and pH-responsiveness properties. Eur. Polym. J. 40 (7), 1399–1407. https://doi.org/10.1016/j.eurpolymj.2004.01.039. Jul.

Mahmoud, M.A., 2014. Evaluating the damage caused by calcium sulfate scale precipitation during low- and high-salinity-water injection. J. Can. Pet. Technol. 53 (3), 141–150. https://doi.org/10.2118/164634-PA.

Mignon, A., De Belie, N., Dubruel, P., Van Vlierberghe, S., 2019. Superabsorbent polymers: a review on the characteristics and applications of synthetic, polysaccharide-based, semi-synthetic and 'smart' derivatives. Eur. Polym. J. 117, 165–178. https://doi.org/10.1016/j.eurpolymj.2019.04.054. Aug.

Negi, H., Verma, P., Singh, R.K., 2021. A comprehensive review on the applications of functionalized chitosan in petroleum industry. Carbohydr. Polym. 266, 118125 https://doi.org/10.1016/j.carbpol.2021.118125. Aug.

Oppong, S.A., Mandal, M., Ojha, K., 2022. Synthesis and optimization of bentonite enforced poly (acrylamide/co- sodium dodecylbenzensulfonate) preformed particle gels for conformance control in high salinity reservoirs. Petrol. Sci. Technol. 1–18. https://doi.org/10.1080/10916466.2022.2063333. Apr.

Oppong, S.A., Mandal, M., Ojha, K., 2023. Synthesis and optimization of bentonite enforced poly (acrylamide/co- sodium dodecylbenzensulfonate) preformed particle gels for conformance control in high salinity reservoirs. Petrol. Sci. Technol. 41 (5), 546–563. https://doi.org/10.1080/10916466.2022.2063333. Mar.

Paprouschi, A., Fatemi, M., Ghazanfari, M.H., 2021. Effect of silicate sodium and graphene nanoplatelets on morphology and rheology characteristics of new synthesized preformed particle gel (PPG) for water shut-off treatment. J. Pet. Sci. Eng. 204, 108736 https://doi.org/10.1016/j.petrol.2021.108736. Sep.

Pu, J., Bai, B., Alhuraishawy, A., Schuman, T., Chen, Y., Sun, X., 2019. A recrosslinkable preformed particle gel for conformance control in heterogeneous reservoirs containing linear-flow features. SPE J. 24 (4), 1714–1725. https://doi.org/10.2118/191697-PA. Aug.

Rani, G.U., Konreddy, A.K., Mishra, S., 2018. Novel hybrid biosorbents of agar: swelling behaviour, heavy metal ions and dye removal efficacies. Int. J. Biol. Macromol. 117, 902–910. https://doi.org/10.1016/j.ijbiomac.2018.05.163.

Reddy, B.R., Eoff, L., Dalrymple, E.D., Black, K., Brown, D., Rietjens, M., 2003. A natural polymer-based cross-linker system for conformance gel systems. SPE J. 8 (2), 99–106. https://doi.org/10.2118/84937-PA. Jun.

Sabadini, R.C., Martins, V.C.A., Pawlicka, A., 2015. Synthesis and characterization of gellan gum: chitosan biohydrogels for soil humidity control and fertilizer release. Cellulose 22 (3), 2045–2054. https://doi.org/10.1007/s10570-015-0590-6. Jun.

Saber-Samandari, S., Gazi, M., Yilmaz, E., 2012a. UV-induced synthesis of chitosan-g-polyacrylamide semi-IPN superabsorbent hydrogels. Polym. Bull. 68 (6), 1623–1639. https://doi.org/10.1007/s00289-011-0643-4.

Saber-Samandari, S., Yilmaz, O., Yilmaz, E., 2012b. Photoinduced graft copolymerization onto chitosan under heterogeneous conditions. J. Macromol. Sci. Part A Pure Appl. Chem. https://doi.org/10.1080/10601325.2012.687970.

Sagbana, P.I., Abushaikha, A.S., 2021. A comprehensive review of the chemical-based conformance control methods in oil reservoirs. J. Pet. Explor. Prod. Technol. 11 (5), 2233–2257. https://doi.org/10.1007/s13202-021-01158-6. May.

Salunkhe, B., Schuman, T., Al Brahim, A., Bai, B., 2021. Ultra-high temperature resistant preformed particle gels for enhanced oil recovery. Chem. Eng. J. 426, 130712 https://doi.org/10.1016/j.cej.2021.130712. Dec.

Seidy Esfahlan, M., Khodapanah, E., Tabatabaei-Nezhad, S.A., 2021. Comprehensive review on the research and field application of preformed particle gel conformance control technology. J. Petrol. Sci. Eng. https://doi.org/10.1016/j.petrol.2021.108440.

Seright, R., Brattekas, B., 2021. Water shutoff and conformance improvement: an introduction. Petrol. Sci. 18 (2), 450–478. https://doi.org/10.1007/s12182-021-00546-1. Apr.

Shamlooh, M., Hussein, I.A., Nasser, M.S., Magzoub, M., Salehi, S., 2020. Development of pH-controlled aluminum-based polymeric gel for conformance control in sour gas reservoirs. ACS Omega 5 (38), 24504–24512. https://doi.org/10.1021/acsomega.0c02967. Sep.

Shamlooh, M., Elaf, R., Hussein, I.A., Saad, M., Bai, B., 2022. Chitosan/polyacrylamide green gels for water control in high-temperature reservoirs. Energy Fuel. 36 (7), 3816–3824. https://doi.org/10.1021/acs.energyfuels.2c00242. Apr.

Sohail, M., Ahmad, M., Minhas, M.U., Ali, L., Khalid, I., Rashid, H., 2015. Controlled delivery of valsartan by cross-linked polymeric matrices: synthesis, in vitro and in vivo evaluation. Int. J. Pharm. 487 (1–2), 110–119. https://doi.org/10.1016/j.ijpharm.2015.04.013. Jun.

Sun, L., et al., 2019. Water plugging performance of preformed particle gel in partially filled fractures. Ind. Eng. Chem. Res. 58 (16), 6778–6784. https://doi.org/10.1021/acs.iecr.9b00128. Apr.

Sun, X., Bai, B., Long, Y., Wang, Z., 2020. A comprehensive review of hydrogel performance under CO2 conditions for conformance control. J. Pet. Sci. Eng. 185, 106662 https://doi.org/10.1016/j.petrol.2019.106662. Feb.

Taha, A., Amani, M., 2019. Overview of water shutoff operations in oil and gas wells; chemical and mechanical solutions. ChemEngineering 3 (2), 51. https://doi.org/10.3390/chemengineering3020051. May.

Tongwa, P., Bai, B., 2014. Degradable nanocomposite preformed particle gel for chemical enhanced oil recovery applications. J. Pet. Sci. Eng. https://doi.org/10.1016/j.petrol.2014.10.011.

Wang, L., Long, Y., Ding, H., Geng, J., Bai, B., 2017. Mechanically robust re-crosslinkable polymeric hydrogels for water management of void space conduits containing reservoirs. Chem. Eng. J. 317, 952–960. https://doi.org/10.1016/j.cej.2017.02.140. Jun.

Yang, Y., Peng, W., Zhang, H., Wang, H., He, X., 2022. The oil/water interfacial behavior of microgels used for enhancing oil recovery: a comparative study on microgel powder and microgel emulsion. Colloids Surfaces A Physicochem. Eng. Asp. 632, 127731 https://doi.org/10.1016/j.colsurfa.2021.127731. Jan.

Zhou, C., Wu, Q., 2011. A novel polyacrylamide nanocomposite hydrogel reinforced with natural chitosan nanofibers. Colloids Surf. B Biointerfaces 84 (1), 155–162. https://doi.org/10.1016/j.colsurfb.2010.12.030. May.